

# A 3D FE Modeling of Machining Process of Nomex® Honeycomb Core: Influence of the Cell Structure Behaviour and Specific Tool Geometry

M Jaafar, S Atlati, H Makich, M Nouari, A Moufki, B Julliere

## ► To cite this version:

M Jaafar, S Atlati, H Makich, M Nouari, A Moufki, et al.. A 3D FE Modeling of Machining Process of Nomex® Honeycomb Core: Influence of the Cell Structure Behaviour and Specific Tool Geometry. *Procedia CIRP, ELSEVIER*, 2017, 58, pp.505 - 510. 10.1016/j.procir.2017.03.255 . hal-03325725

HAL Id: hal-03325725

<https://hal.univ-lorraine.fr/hal-03325725>

Submitted on 25 Aug 2021

**HAL** is a multi-disciplinary open access archive for the deposit and dissemination of scientific research documents, whether they are published or not. The documents may come from teaching and research institutions in France or abroad, or from public or private research centers.

L'archive ouverte pluridisciplinaire **HAL**, est destinée au dépôt et à la diffusion de documents scientifiques de niveau recherche, publiés ou non, émanant des établissements d'enseignement et de recherche français ou étrangers, des laboratoires publics ou privés.

16<sup>th</sup> CIRP Conference on Modelling of Machining Operations

## A 3D FE modeling of machining process of Nomex® honeycomb core: influence of the cell structure behaviour and specific tool geometry

M. Jaafar<sup>a</sup>, S. Atlati<sup>a</sup>, H. Makich<sup>a\*</sup>, M. Nouari<sup>a</sup>, A. Moufki<sup>a</sup>, B. Julliere<sup>b</sup>

<sup>a</sup>University of Lorraine, Laboratoire d'Énergétique et de Mécanique Théorique et Appliquée, LEMTA CNRS-UMR 7563, Mines Albi, Mines Nancy, GIP-InSIC, 27 rue d'Heilleule, 88100 Saint-Dié-des-Vosges, France

<sup>b</sup>Evatec-Tools, 12 rue des Terres Rouges - Z.I. Metzange - F - 57100, Thionville, France

\* Corresponding author. Tel.: +33 (0)329 421 821; fax: +33 (0)329 421 825. E-mail address: [hamid.makich@univ-lorraine.fr](mailto:hamid.makich@univ-lorraine.fr)

### Abstract

This paper deals with the numerical simulation of the honeycomb machining process taking into account the behaviour of Nomex® material and the effect of its cell structure. Using Hashin failure criterion, a single orthotropic layer model was developed to simulate the machining of honeycomb structure. To understand the effect of the cutting parameters on machinability of these materials, the interaction between a specific cutting tool geometry and the structure walls has been analyzed. The results of the 3D FE simulations developed for milling process of honeycomb materials show the evolution of cutting forces and surface quality generated during machining the Nomex® honeycomb.

© 2017 The Authors. Published by Elsevier B.V. This is an open access article under the CC BY license (<http://creativecommons.org/licenses/by/4.0/>).

Peer-review under responsibility of the scientific committee of The 16th CIRP Conference on Modelling of Machining Operations

*Keywords:* Honeycomb; Nomex; Milling; Modelling

### 1. Introduction

Nomex® honeycomb structures are characterized by a combination of lightweight and high compressive out-of-plane strength. Nomex® is considered as a good candidate for aircraft and aerospace applications due to their thermal resistance, good insulating properties and low dielectric properties. Nomex® honeycomb material is used as the core for sandwich structures. Combined with aluminum or composite face sheet, they formed a good sandwich material used, for example, in aircraft floors, doors, wing flaps and rudders [1]. These uses require the shaping of the honeycomb core to adapt it. Nevertheless, this material presents a forming challenge, three specific characteristics of Nomex® honeycomb causes machining difficulties: it is made of a composite material and constituted by aramid fibers and phenolic resin, the thin thickness of these walls and its cell geometry. To resolve these problems, the use of a third body as frozen water or thermosetting resin is recommended in the literature to solidify the structure and avoid deformation and vibration of cells. However, these methods

generate additional cost and an important time of implementation. There are only few previous studies showing the influence of cutting conditions on the machinability of this kind of materials. The optimization of the machining process of the honeycomb structures still is quite confidential. The optimization must go through a step of understanding the interactions that occur during honeycomb milling. The FE modelling seems to be more adequate to follow the local phenomena that occur during shaping.

Many researchers have proposed a finite element modelling of impact on the honeycomb structure or on out-of-plane compression. Two methods are used to model the honeycomb behavior, the first is based on the homogenization of the structure to study the mechanical behavior of the structure under different loads [2], the second model replicates the real geometry of the honeycomb structure by the presentation of the cells to get more information on the deformation of cells and walls inside the honeycomb structure.

Knowing that the honeycomb walls are composed of Nomex® paper (aramid fibers and phenolic resin), four

modeling approaches exist. The first consist to assign isotropic behavior at the walls of the honeycomb with an elastic–plastic properties [3–7]. This model is easy to setup; however, it neglects the composite architecture of the Nomex® paper. The second method represents a single layer orthotropic Nomex® paper modelling, which represents more possibilities of Nomex® paper modelling [8–12]. In the third approach, Nomex® paper is modelled using a multi-layer structure by the representation of three layers with an isotropic behavior for phenolic resin coating, two layers of this resin envelope the aramid paper, this latter can be modelled as an isotropic or orthotropic material, [11, 13, 14]. Lastly, Nomex® paper is modelled using a multi-layer structure with the addition of the resin accumulation in the hexagon corners of the cells. All these studies treat the mechanical behavior of honeycomb structures under mechanical stress such as out-of-plane compression, shear and impact loading.

The honeycomb core machining is confronted in the same way as the conventional composites materials to the problem of the induced damage during the chip formation process. Many failure criteria are proposed for composite structures [15]. Firstly, we find no-interactive failure criteria [16] which are divided into two parts: the maximum stress law and strain criterion. These two criteria consider that the composite fails when the stress or the strain exceed the respective allowable, being a simple and direct way to predict failure of composites. Secondly, we find interactive failure criteria [16] which account for interactions between the different stresses, Tsai-Wu and Tsai-Hill are the most well-known criteria. Finally, separate mode criteria [16] which separate the fibers and matrix controlled failure modes. Hashin criteria is one of these criteria.

In this study, FE modelling of the honeycomb cutting process is proposed to study the honeycomb structure and the effect of cutting parameters on the machinability of this kind of materials.

## 2. Numerical modelling

### 2.1. Finite element model

The numerical model for the honeycomb milling was developed using the finite element code ABAQUS/EXPLICIT. The workpiece is made of Nomex® honeycomb structure with a density of 48 kg/m<sup>3</sup>, constituted by hexagonal cells with size of 3.2 mm. Table 1 summarizes the main geometric characteristics of the workpiece. To analyze the interaction of the honeycomb core with the milling cutter, the modelled structure is composed by 10 × 8 cells rows (Figure 1.a). The honeycomb core was modelled using shell elements (S4R) with hourglass-control and element deletion. The elements size is taken about 5 μm.

The developed model takes into account the orthotropic property of Nomex® paper cited above. As the mechanical properties are different following the considered directions, it is necessary to take into account the orientations of Nomex® paper in the hexagonal cells. Thereby, a local reference mark has been defined for each cells walls orientation (Figure 1.b). Three local orientations are designed, an orientation for double

wall, an orientation for the first single wall and an orientation for the second single wall.

Table 1. Geometrical characteristics of honeycomb core.

Honeycomb designation	Density [Kg/m <sup>3</sup> ]	Cell size l [mm]	Wall size t [mm]	Angle $\alpha$ [°]
A10-48-3	48	3.2	0.06	120

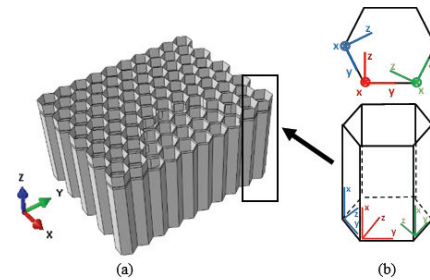
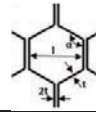


Fig. 1. (a) Nomex® honeycomb modeling, (b) local cell wall orientation.

The milling cutter used in our investigations is specific tool with two parts. The first part is a cutter body made of high speed steel with 16 mm in diameter and having ten helix with chip breaker. This tool part is designated by hogger. The second part is a circular cutting blade made of tungsten carbide with a diameter of 18.3 mm and having a rake angle of 22° and a flank angle of 2.5°. A rigid and discrete behaviour was attributed for the cutting tool. Then, a reference point RP was defined at the tool center in order to apply machining condition; spindle speed and feed speed (figure 2)

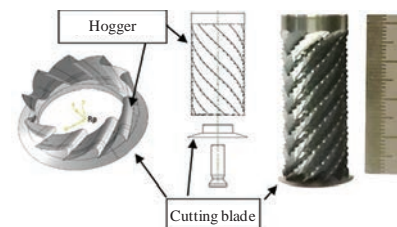


Fig. 2. Milling cutter for Nomex® honeycomb core.

Concerning the contact, firstly, the contact interface between the tool and the honeycomb is defined by a surface-to-surface contact with penalty contact method. Secondly, the contact that occurs between the honeycomb walls is also modeled by assigning it a general contact with the penalty contact method. Also, in this model the mechanical contact is considered and for the normal contact we used a hard contact and for the tangential contact we used the well-known Coulomb law.

In order to reduce the CPU time, an initial tool engagement was defined. The aim is to ensure a complete contact between the tool and the material structure from the simulation beginning. Moreover, the initial engagement is designed in consideration of the particular geometry of the two parts of the milling cutter (Figure 3).

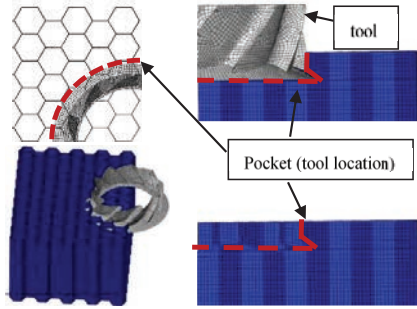


Fig. 3. Initial tool engagement in honeycomb workpiece.

2.2. Prediction of the honeycomb cells damage

The developed 3D FE model is based on the modelling of the orthotropic single layer. This approach is based on the homogenized proprieties of the Nomex® composite paper (aramid fiber and phenolic resin). This orthotropy is represented by a difference of mechanical behavior of Nomex® paper on each direction,[8]. For these reasons, a local orientation was attributed to each cell wall. Considering typical paper fabrication, the Nomex® paper has more fibers aligned in the roll direction [7, 9] and [12]. This gives a higher resistance in this direction. Heimbs et al. [17] have determined the mechanical characteristics of the Nomex® paper behaviour (Table 2). We considered these characteristics for the mechanical behavior of our Nomex® material model.

Table 2. Mechanical properties of Nomex® paper used in the numerical modelling [15,17].

Mechanical properties	Values
Longitudinal stiffness, E1 (MPa)	32500
Transverse stiffness, E2 (MPa)	30900
Through-the-thickness stiffness, E3 (MPa)	30900
Poisson's ratios, ν12, ν13, ν23	0.083
Shear modulus, G12, G13, G23 (MPa)	1900
Longitudinal tensile strength: Xt (Mpa)	578
Longitudinal compressive strength: Xc (Mpa)	205
Transverse tensile strength: Yt (Mpa)	498
Transverse compressive strength: Yc (Mpa)	204
In-plan shear strength: S (Mpa)	95
Density, ρ g/cm3	1.3

Due to the orthotropic behaviour of the workpiece, the 3D Hashin criterion [3, 18] was chosen to predict the damage initiation and evolution inside the Nomex® paper. Hashin criteria was chosen because it takes into account the interaction between the different stress components. The Hashin criterion is defined for each cell wall orientation as follow:

- 1-direction tensile fracture:  $\sigma_{11} \geq 0$ ,  
 $\sigma_{11} = X_t$
- 1-direction compressive fracture :  $\sigma_{11} < 0$   
 $\sigma_{11} = X_c$
- 2-direction tensile failure:  $(\sigma_{22} + \sigma_{33}) \geq 0$

$$\frac{(\sigma_{22} + \sigma_{33})^2}{Y^2} + \frac{\sigma_{12}^2 + \sigma_{13}^2 + \sigma_{23}^2 - \sigma_{22}\sigma_{33}}{S^2} = 1$$

2-direction compressive failure:  $(\sigma_{22} + \sigma_{33}) < 0$

$$\frac{1}{Y_c} \left[ \left( \frac{Y_c}{2S} \right)^2 - 1 \right] (\sigma_{22} + \sigma_{33}) + \frac{(\sigma_{22} + \sigma_{33})^2}{4S^2} + \frac{\sigma_{12}^2 + \sigma_{13}^2 + \sigma_{23}^2 - \sigma_{22}\sigma_{33}}{S^2} = 1$$

where the  $\sigma_{ij}$  terms are the components of the stress tensor.

3. Results and discussion

The aim of the modelling of honeycomb structures milling operation is to study the interaction between the structure and the tool behaviour when machining cells honeycomb. In order to validate our model, several experimental milling tests have been performed on Nomex® honeycomb and a comparison of the obtained cutting forces was carried out.

3.1. FE model validation

To allow a comparison of experimental and simulated results, milling tests were carried out on a three-axis machining center (Figure 4), with a maximum spindle speed 24000 rpm. The cutting forces were measured using Kistler dynamometer model 9129AA and its charge amplifier 5070A. The direction of the honeycomb double walls coincides with the x-direction of the Kistler dynamometer and the feed direction of the milling machine. To perform the comparison between the numerical and experimental results, two feed speeds and three spindle speeds were chosen. The machining conditions are summarized in Table 3.



Fig. 4. Experimental test setup.

Table 3. Machining conditions.

Feed rate (mm/min)	200, 3000
Spindle speed (rpm)	2000, 15000, 23000

3.2. Machining forces analysis

The results obtained from the FE simulations for the milling forces are compared to the experimental one under similar machining parameters. The analysis of numerical results gives us access to the local interactions and thus their influence on

the cutting forces evolution. Figure 5 shows the evolution of the cutting forces during the machining of a honeycomb cell row for a period of 0.24 s. The cell range represents a tool feed of 3.7 mm. In general, the cutting forces generated when machining Nomex® honeycomb are low compared to the machining of the composite or metallic materials. The cutting forces do not exceed 15 N. The low density of the Nomex® structure is the cause of this low level of cutting forces. Often the thrust force is neglected for the milling of composite materials, because it is lower than the other components of the cutting force [19, 20]. However, in our case for the honeycomb machining using the combined tool, the thrust force represents the highest component of the machining forces. This is due to the particular geometry of the milling cutter and the strength of the honeycomb walls in the out-of-plane compression direction.

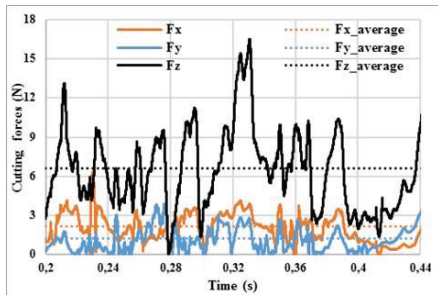


Fig. 5. Numerical cutting forces evolution during the milling of a cells row.

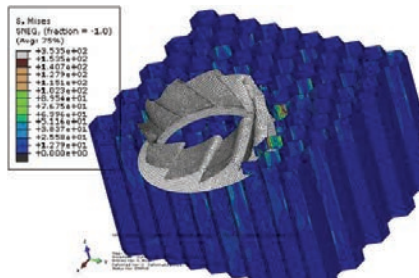


Fig. 6. Distribution of stress on honeycomb walls during machining.

It can be noted from these simulations that the honeycomb machining process is particularly characterized by fluctuations in cutting forces level. This is due to the alveolar structure of the honeycomb which causes vibration of the structure and local cutting dissymmetry. These vibrations generate a stress distribution in all the cell walls of the honeycomb (Figure 6). Figures 7, 8 and 9 show a comparison of the experimental results with those obtained for the machining forces using the 3D model for different feed rates and spindle speeds. The numerical results are in good agreement with those obtained experimentally except the tangential force  $F_y$ . The tangential force remains invariant as a function of the cutting conditions and does not exceed 1.5 N, contrary to the experimental observed forces where a reduction is noticed by increasing the spindle speed. This invariability and low cutting forces can be explained by the suppression elements procedure generated by the failure criterion under lagrangian formulation. The element suppression leads to the contact loss between the saw blade and the honeycomb cells. This leads to the loss of the local elastic

springback of the walls which is responsible to the opposition of the tool rotation, [21, 22].

In a global view, the measured cutting forces show a decrease function of the spindle speed and an increase function of the feed speed (see Figures 7, 8 and 9). This behaviour is a characteristic of machining composite materials, [23]. With low spindle speed (2000 rpm) and high feed rate (3000 mm/min), the cutting tool generates the greatest machining forces.

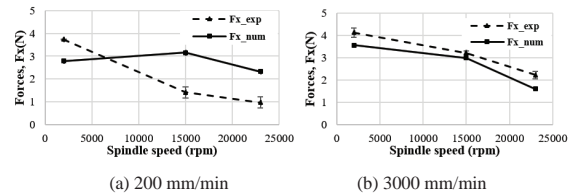


Fig. 7. Evolutions of feed forces,  $F_x$ .

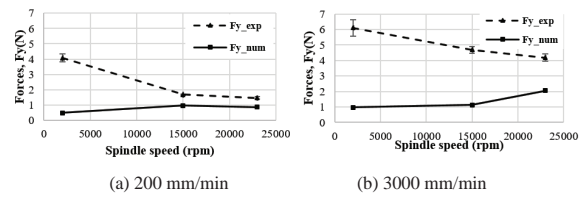


Fig. 8. Evolutions of tangential forces,  $F_y$ .

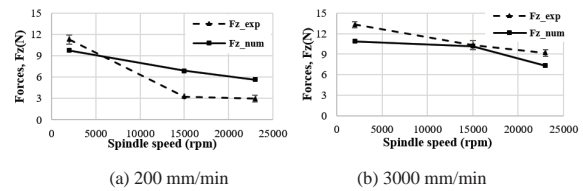


Fig. 9. Evolutions of thrust forces  $F_z$ .

For a fixed feed rate, the increase in the spindle speed decreases the cutting forces. This decrease is greater for a low feed rate (200 mm/min) such that a decrease of 74% is observed for the feed force  $F_x$  and 64% for the tangential force  $F_y$  and 73% for the thrust force  $F_z$  comparing the forces between 2000 rpm and 23000 rpm spindle speeds (Figure 7-a, 8-a and 9-a). A more moderate decrease can be observed for a feed rate of 3000 mm/min with a difference of 46% for  $F_x$ , 31% for  $F_y$  and 31% for  $F_z$  (figures 7-b, 8-b and 9-b).

The numerical analysis of the interactions between the combined tool and the cut walls makes possible to explain the observed trends on the cutting forces. We observe on the FE simulations that the evacuation rate of the cut walls by the tool upper part affects the cutting forces. Figure 10 shows a comparison between the milling process for two different cutting conditions at the same spindle speed and different feed rates. The high feed rate 3000 mm/min (Figure 10-a), produces an accumulation of the cut walls above the saw blade and in front of the hogger causing then an increase in the machining forces level. In the contrary for low feed rate (Figure 10-b), 200 mm/min, a better chip evacuation can be observed with less accumulation of chips on the cutting blade and in front of the

hogger. The reduction of the feed rate allows the tool to better evacuate chips and thus reduce the cutting forces.

Thus, the cutting of the Nomex® honeycomb with this type of cutting tool occurs in three steps. First, the saw blade cut with continuous rubbing the honeycomb walls. In the second step, the end of the cut walls slides on the upper face of saw blade until reaching the hogger. Finally, this hogger with its chip breaker play the role of dismantling the walls.

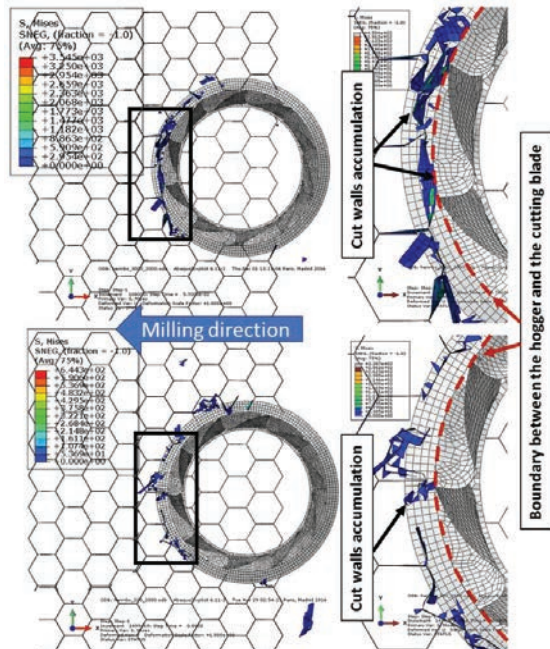


Fig. 10. Effect of the machining conditions on the cell walls chip accumulation. (a)  $f=3000\text{mm/min}$ ,  $N=2000\text{ rpm}$ ; (b)  $f=200\text{mm/min}$ ,  $N=2000\text{ rpm}$ .

### 3.3. Machining surface quality

Given the low level of cutting forces, the quality of the obtained machined surface allows to establish a criterion for determining the machinability of the honeycomb structures. The surface quality depends on the cutting conditions (feed rate and spindle speed), [24, 25]. Delamination, flaking and degradation of the matrix are the major damage modes observed on the composite materials, [26, 27]. For the Nomex® honeycomb material, two main modes of surface damage are observed (Figure 11); uncut aramid fibers along the machined surface and tearing of the walls. The appearance of the uncut fibers is a machining defect specific to the composite material which depends on the type of the fibers and their orientation [21]. The tearing of Nomex® paper, linked to the cellular appearance of the honeycomb structure, occurs under the effect shear loading, [28, 29].

The uncut fibers are observed for low spindle speeds (Figure 11-a and 11-c). However, the high feed rate affects directly the tearing of the honeycomb walls. The advancement of the tool creates the folding of the thin walls of the Nomex until tearing.

It is well known that the surface quality is of paramount importance for the use of the Nomex® honeycomb in sandwich materials. The machining defects cause a reduction of bond strength between the skin and the honeycomb core, and thus a weaker joint for composite sandwich structures, [30, 31].

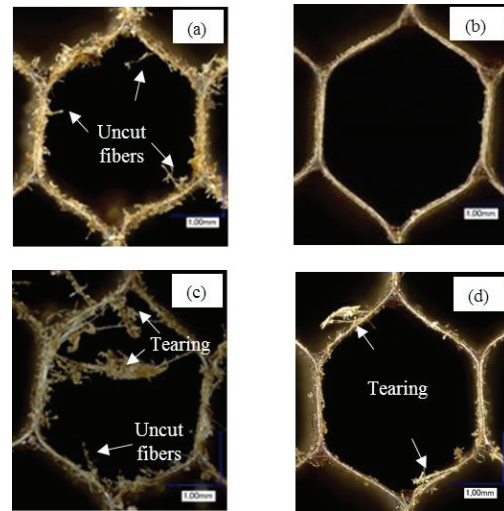


Fig. 11. Honeycomb machining surfaces. (a)  $f=200\text{ mm/min}$ ,  $N=2000\text{ rpm}$ ; (b)  $f=200\text{ mm/min}$ ,  $N=23000\text{ rpm}$ ; (c)  $f=3000\text{ mm/min}$ ,  $N=2000\text{ rpm}$ ; (d)  $f=3000\text{ mm/min}$ ,  $N=23000\text{ rpm}$ .

### 4. Conclusion

In this work, 3D FE modeling of the milling operation was performed on the honeycomb structures. The proposed model takes into account the complex interactions between the cellular structure of the workpiece and the specific tools used for machining this kind of materials. The orthotropic behaviour of the honeycomb material is considered for the separation of materials during machining. The Hashin failure criterion was used according to the direction and the loading type encountered by the Nomex® material.

Experimental tests were carried out and compared to the numerical results. The numerical simulations show an evolution of the forces in a good agreement with the experimental results except for the tangential force. The letter shows a constant evolution with the cutting conditions. This behavior is due to the “delete elements technique” with the Hashin failure criterion.

Nevertheless, the 3D FE allows to analyze finely the interactions between the honeycomb structure and the milling cutter according to the machining conditions. This can be a helpful method to optimize the tool geometry and the quality of the machined surface. In order to reduce the accumulation of the cut walls ahead the upper part of tool and improve surface quality, other geometries of cutting tool will be studied in forthcoming works.

### Acknowledgements

The authors wish to express their thanks and appreciation to members of the following organizations for their support:

- The French National Research Agency (ANR) for supporting the 'LARIOPAC LabCom' project under following number ANR-13-LAB2-0002.
- The industrial partner 'Evatec-tools Group'

## References

- [1] D. GAY, *Matériaux composites*, Hermes, 2015.
- [2] P. Taylor, A. K. Pickett, A. J. Lamb, and F. Chaudoye, "Materials characterisation and crash modelling of composite-aluminium honeycomb sandwich material," no. February 2015, pp. 37–41, 2009.
- [3] C. C. Foo, G. B. Chai, and L. K. Seah, "A model to predict low-velocity impact response and damage in sandwich composites," *Compos. Sci. Technol.*, vol. 68, pp. 1348–1356, 2008.
- [4] Á. J. Mancha, "Ingeniero industrial optimization of lightweight sandwich structures of commercial aircraft interior parts subjected to low-velocity impact," Universidad Pontificia Comillas MADRID, 2012.
- [5] I. Ivañez and M. M. Moure, "The oblique impact response of composite sandwich plates," *Compos. Struct.*, vol. 133, pp. 1127–1136, 2015.
- [6] Z. Shengqing and C. G. Boay, "Damage and failure mode maps of composite sandwich panel subjected to quasi-static indentation and low velocity impact," *Compos. Struct.*, vol. 101, pp. 204–214, 2013.
- [7] R. Roy, J. H. Kweon, and J. H. Choi, "Meso-scale finite element modeling of Nomex honeycomb cores," *Adv. Compos. Mater.*, vol. 23, no. 1, pp. 17–29, 2014.
- [8] R. Seemann and D. Krause, "Numerical Modeling of Nomex Honeycomb Sandwich Cores at Meso-Scale Level," *Compos. Struct.*, no. September, 2016.
- [9] R. Roy, S. Park, J. Kweon, and J. Choi, "Characterization of Nomex honeycomb core constituent material mechanical properties," *Compos. Struct.*, vol. 117, pp. 255–266, 2014.
- [10] S. Heimbs, "Virtual testing of sandwich core structures using dynamic finite element simulations," *Comput. Mater. Sci.*, vol. 45, no. 2, pp. 205–216, 2009.
- [11] S. Fischer, K. Drechsler, S. Kilchert, and A. Johnson, "Mechanical tests for foldcore base material properties," *Compos. Part A*, vol. 40, no. 12, pp. 1941–1952, 2009.
- [12] R. Roy, K. H. Nguyen, Y. B. Park, J. H. Kweon, and J. H. Choi, "Testing and modeling of Nomex TM honeycomb sandwich Panels with bolt insert," *Compos. Part B*, vol. 56, pp. 762–769, 2014.
- [13] S. V. Kilchert, "Nonlinear finite element modelling of degradation and failure in folded core composite sandwich structures," Universität Stuttgart, 2013.
- [14] R. SEEMANN and D. KRAUSE, "Numerical modelling of nomex honeycomb cores for detailed analyses of sandwich panel joints," 11th World Congr. Comput. Mech. (WCCM).
- [15] C. T. Sun, B. J. Quinn, and J. Tao, "Comparative Evaluation of Failure Analysis Methods for Composite Laminates," 1996.
- [16] G. M. Newaz and R. F. Gibson, *Proceedings of the eighth japan-us conference on composite materials*. CRC Press LLC, 1998.
- [17] S. Heimbs, J. Cichosz, M. Klaus, S. Kilchert, and A. F. Johnson, "Sandwich structures with textile-reinforced composite foldcores under impact loads," *Compos. Struct.*, vol. 92, no. 6, pp. 1485–1497, 2010.
- [18] Z. Hashin, "Failure Criteria for Unidirectional Fiber Composites," *J. Appl. Mech.*, vol. 47, no. June, pp. 329–334, 1980.
- [19] D. Geng, D. Zhang, Y. Xu, F. He, D. Liu, and Z. Duan, "Rotary ultrasonic elliptical machining for side milling of CFRP: Tool performance and surface integrity," *Ultrasonics*, vol. 59, pp. 128–137, 2015.
- [20] M. Ucar and Y. Wang, "End-milling machinability of a carbon fiber reinforced laminated composite," *J. Adv. Mater.*, vol. 37, no. 4, pp. 46–52, 2005.
- [21] X. M. Wang and L. C. Zhang, "An experimental investigation into the orthogonal cutting of unidirectional fibre reinforced plastics.pdf," *Int. J. Mach. Tools Manuf.*, vol. 43, pp. 1015–1022, 2003.
- [22] L. Lasri, M. Nouari, and M. El Mansori, "Modelling of chip separation in machining unidirectional FRP composites by stiffness degradation concept," *Compos. Sci. Technol.*, vol. 69, no. 5, pp. 684–692, 2009.
- [23] M. P. Jenarathanan and R. Jeyapaul, "Optimisation of machining parameters on milling of GFRP composites by desirability function analysis using Taguchi method," vol. 5, no. 4, pp. 23–36, 2013.
- [24] M. Haddad, R. Zitoune, F. Eyma, and B. Castanie, "Study of the surface defects and dust generated during trimming of CFRP: Influence of tool geometry, machining parameters and cutting speed range," *Compos. Part A*, vol. 66, pp. 142–154, 2014.
- [25] J. P. Davim, P. Reis, and C. Conceic, "A study on milling of glass fiber reinforced plastics manufactured by hand-lay up using statistical analysis (ANOVA) ao Ant o," vol. 64, pp. 493–500, 2004.
- [26] R. Zitoune, M. El Mansori, and V. Krishnaraj, "Tribo-functional design of double cone drill implications in tool wear during drilling of copper mesh/CFRP/woven ply," *Wear*, vol. 302, no. 1–2, pp. 1560–1567, Apr. 2013.
- [27] S. Zenia, L. Ben Ayed, M. Nouari, and A. Delamézière, "An elastoplastic constitutive damage model to simulate the chip formation process and workpiece subsurface defects when machining CFRP composites," *Procedia CIRP*, vol. 31, pp. 100–105, 2015.
- [28] Y. Aminanda, "Contribution à l'analyse et à la modélisation de structures sandwichs impactées," L'ÉCOLE NATIONALE SUPÉRIEURE DE L'AÉRONAUTIQUE ET DE L'ESPACE, 2004.
- [29] L. Liu, H. Wang, and Z. Guan, "Experimental and numerical study on the mechanical response of Nomex honeycomb core under transverse loading," *Compos. Struct.*, vol. 121, pp. 304–314, 2015.
- [30] J. Rion, Y. Leterrier, and J. E. Manson, "Prediction of the adhesive fillet size for skin to honeycomb core bonding in ultra-light sandwich structures," *Compos. Part A*, vol. 39, pp. 1547–1555, 2008.
- [31] H. Tchoutouo and N. Gandy, "Adhesiveless Honeycomb Sandwich Structure With Carbon Graphite Prepreg for Primary Structural Application: a Comparative Study To the Use of Adhesive Film," no. May, 2012.